



Heterogeneous photocatalysis of tris(2-chloroethyl) phosphate by UV/TiO₂: Degradation products and impacts on bacterial proteome



Jinshao Ye ^{a,b}, Juan Liu ^a, Chongshu Li ^a, Pulin Zhou ^a, Shuang Wu ^a, Huase Ou ^{a,*}

^a School of Environment, Guangzhou Key Laboratory of Environmental Exposure and Health, and Guangdong Key Laboratory of Environmental Pollution and Health, Jinan University, Guangzhou 510632, China

^b Joint Genome Institute, Lawrence Berkeley National Laboratory, Walnut Creek 94598, CA, USA

ARTICLE INFO

Article history:

Received 21 April 2017

Received in revised form

27 June 2017

Accepted 15 July 2017

Available online 18 July 2017

Keywords:

Organophosphorus flame retardant

Photocatalysis

Proteomics

Water treatment

Dechlorination

ABSTRACT

The widespread, persistent and toxic organophosphorus esters (OPEs) have become one category of emerging environmental contaminants. Thus, it is in urgent need to develop a cost-effective and safe treatment technology for OPEs control. The current study is a comprehensive attempt to use UV/TiO₂ heterogeneous photocatalysis for the degradation of a water dissolved OPEs, tris(2-chloroethyl) phosphate (TCEP). A pseudo-first order degradation reaction with a k_{obs} of 0.3167 min⁻¹ was observed, while hydroxyl radical may be the dominating reactive oxidative species. As the reaction proceeded, TCEP was transformed to a series of hydroxylated and dechlorinated products. The degradation efficiency was significantly affected by pH value, natural organic matters and anions, implying that the complete mineralization of TCEP would be difficult to achieve in actual water treatment process. Based on the proteomics analysis regarding the metabolism reactions, pathways and networks, the significant activation of transmembrane transport and energy generation in *Escherichia coli* exposed to preliminary degrading products suggested that they can be transported and utilized through cellular metabolism. Furthermore, the descending trend of stress resistance exhibited that the toxicity of products was obviously weakened as the treatment proceeded. In conclusion, hydroxylation and dechlorination of TCEP with incomplete mineralization were likewise effective for its detoxification, indicating that UV/TiO₂ will be an alternative treatment method for OPEs control.

© 2017 Elsevier Ltd. All rights reserved.

1. Introduction

Organophosphorus esters (OPEs) are chemicals applied as annexing agents in a variety of industrial products, such as building materials, automobile components, paint, film, shoes and tires, to protect or to enhance their fire resistance and thermostability (Reemtsma et al., 2008). Especially, after the prohibition of poly-brominated biphenyl ethers flame retardants, the application of OPEs as alternative flame retardants increased rapidly. The widespread usage of OPEs resulted in their diffusion from host materials into water, air and soil. Furthermore, the persistence and toxicity of OPEs made them become one category of emerging environmental contaminants (van der Veen and de Boer, 2012; Wei et al., 2015). Recently, the undesired occurrence of some OPEs in natural water sources (Wolschke et al., 2015) and finished drinking water

(Stackelberg et al., 2004) was reported, implying that traditional drinking water and wastewater treatment processes were ineffectual for OPEs removal. Therefore, it is in urgent need to develop cost-effective and safe treatment techniques for OPEs.

In the past few decades, worldwide researchers attempted to apply kinds of advanced oxidation processes (AOPs), including ozonation, photochemical oxidation, electrochemical oxidation and ultrasonic oxidation, for the elimination of organic contaminants (Kasprzyk-Hordern et al., 2003; Pillai et al., 2015). Some ultraviolet driving AOPs (UV-AOPs), especially UV/TiO₂ photocatalysis, have shown a great potential as low-cost, environmental-friendly and sustainable control technologies for persistent organic contaminants in water/wastewater treatment. However, dedicated exploration about the potential application of UV-AOPs for OPEs elimination has only started. It was verified that the degradation of OPEs by UV/H₂O₂ or UV photocatalysis followed pseudo-first-order dynamics (Antonopoulou et al., 2016; Ruan et al., 2013), while Santoro et al. used computational fluid dynamics to simulate the oxidation processes of a common OPE, tris(2-chloroethyl) phosphate (TCEP), in

* Corresponding author.

E-mail address: touhuase@jnu.edu.cn (H. Ou).

two different photoreactors (Santoro et al., 2010). It was reported that a portion of OPEs degrading products after UV/H₂O₂ treatment would become available carbon sources for bacterial growth (Watts and Linden, 2008); furthermore, it was reported that UV/H₂O₂ was more efficient than ozonation for OPEs degradation in a municipal secondary effluent (Yuan et al., 2015). More recently, Alvarez-Corena et al. (2016) used UV/TiO₂ for the multiple degradation of five contaminants, including TCEP, while Antonopoulou et al., (2017) found that UV-vis driving N-doped TiO₂ had a high degradation efficiency for tris (1-chloro-2-propyl) phosphate (TCPP). However, there is little information about the detailed mechanism and pathway in the degradation of OPEs using UV/TiO₂, not to mention the environmental safety of degrading products.

In actual water treatment, a full mineralization of specific targeted organic contaminants will expend a large amount of energy and/or chemical agents. Other coexisting contaminants in natural water, such as natural organic matter (NOM), anions and particulate matter, may become potential competitors of targeted contaminants to consume excess non-selective hydroxyl radical ($\cdot\text{OH}$) (Dodd et al., 2009). Therefore, the incomplete degradation of targeted contaminant (e.g. OPEs) would become an ordinary state in UV/TiO₂ application, with the generation of various intermediate products. Since OPEs are composed of a phosphorus center and three peripheral chemical groups, such as phenyl, alkyl or halohydrocarbon, etc. (Bergman et al., 2012), their degrading products may include halogen disinfecting by-products with high toxicity potential, or phosphorus components which may be utilized by microorganisms. However, the toxicity and bioavailability of these incomplete degrading products were still unknown. Thus, the system-level understanding of the molecular structure and related genetic risks about these incomplete degrading products pose to structural, functional and evolutionary properties of biomolecules will be essential for the evaluation of treatment efficiency and degree.

To date, the toxicological evaluation of OPEs was limited in several traditional techniques, such as water flea test (Waijers et al., 2013), zebrafish test (Kim et al., 2015), cell line test (Ta et al., 2014) and *Vibrio fischerii* bioluminescence test (Antonopoulou et al., 2016). Even these approaches can prove the safety of OPEs at cellular level, it is unnecessary means that OPEs have no negative impacts at molecular network and phylogenetic level. The interactions between OPEs and biomolecules may involve the collective reactions and regulations of biomolecule replication, transcription and translation. Therefore, the safety evaluation of OPEs degradation process will require an investigation in the perspective of protein and metabolism networks. Recently, the novel isobaric tags for relative and absolute quantitation (iTRAQ) labeling quantitative proteomic technology can identify, characterize and quantify protein expression of a specific organism under given conditions. In our previous studies, iTRAQ proteome analysis was used to evaluate the toxicity of degrading products from ciprofloxacin and TCEP (Ou et al., 2017; Ye et al., 2016). The potential findings in regard to the biological and phylogenetic effects of degrading intermediates on protein network will be informative with respect to the regulation of reaction extent from complete mineralization to a moderate degradation, which can reduce the energy and chemical consumption.

In the current study, the degradation of TCEP was explored using 254 nm UV/TiO₂. This study was expected to comprehensively evaluate: (1) the degradation efficiency of TCEP using UV/TiO₂, (2) related degrading pathway and intermediate products, (3) the biological effects of intermediate mixture on model organism at molecular and metabolic network levels, (4) the impacts of coexisting contaminants and natural water matrix on degradation efficiency. In the end, a preliminary assessment of the energy consumption was performed.

2. Materials and methods

2.1. Chemical reagents and strain

All chemical reagents in the current study were of the highest purity available (Text S1).

2.2. UV irradiation device and degradation experiments

A pseudo-parallel UV irradiation device was designed and assembled (Fig. S1). The maximum UV emission peak of the low-pressure mercury lamp (power 8 W, effective length 24 cm, Philips, Holland) was 254 nm. The average irradiating intensity was adjusted to 5.6 mW cm⁻² on the surface of reaction solution (measured by a HAAS-3000 light spectrum irradiation meter, Everfine, China). The reactor vessel was a customized circular quartz vessel with a maximum volume of 120 mL. Before reactions, specific volume of TCEP solution was added into the reactor vessel. In the UV/TiO₂ experiments, the initial concentration of TiO₂ was set in the range of 175–1750 μM (14–140 mg L⁻¹). The solution was maintained at 25 ± 2 °C, pH = 6.8–7.2 (if not be specified), and its uniformity was achieved by shaking the dish at 60 r min⁻¹. At a pre-defined time, 20 mL of the sample was obtained and filtrated by a 0.22 μm polyether sulfone filter, and then was transferred into brown amber tubes (stored at 4 °C) before analysis. The water-only, UV-only and TiO₂-only (adsorption) control experiments were also performed. Tert-butyl alcohol (TBA) and ethyl alcohol (EtOH) were used as scavengers of $\cdot\text{OH}$. Solution pH was adjusted by pH buffered solution, which contains different concentration combinations of NaOH, KH₂PO₄ and H₃PO₄. In the influence factor experiments, the predetermined amount of NaCl (Cl⁻), NaNO₃ (NO₃⁻) or humic acid was added into the solution matrix.

2.3. Quantitative analysis of TCEP and qualitative analysis of intermediate products

The determination of organic intermediate products was conducted using a TripleTOF 5600 + high resolution mass spectrum (HRMS) (Applied Biosystems SCIEX, USA). The quantitative analysis of TCEP was performed using a high performance liquid chromatography with a tandem mass spectrometer (HPLC/MS², TripleQuad 5500, Applied Biosystems SCIEX, USA). Only the relative intensities (peak areas) of organic intermediate products were acquired by HPLC/MS² due to the lack of standard samples. The detailed analysis procedure is presented in Text S2, Tables S1 and S2. The determination of Cl⁻ and PO₄³⁻ was performed using an ICS-2500 analyzer (Dionex, USA) with an ED50A detector. A DIONEX IonPac[®] AS15 column was used with 30.0 mM NaOH solution as the mobile phase. Furthermore, the total organic carbon (TOC) was measured using a Liquid TOC trace analyzer (Elementar, Germany).

2.4. Proteomics analysis

The proteomics analysis included four stages: (1) exposure to targeted contaminants, (2) protein digestion, (3) iTRAQ labeling, and (4) polypeptide analysis using a TripleTOF 5600 + HRMS equipped with a Nanospray III source and a NanoLC 400 system (Applied Biosystems SCIEX, USA). Samples for proteomics analysis included: (1) 60 mL 3.5 μM TCEP solution, (2) 60 mL UV/TiO₂ treated sample #1 (UV/TiO₂ intermediate mixture #1, reaction time = 10 min), (3) 60 mL UV/TiO₂ treated sample #2 (UV/TiO₂ intermediate mixture #2, reaction time = 45 min). The reaction condition was: temperature 25 ± 2 °C, pH 6.5–7.2, [TCEP]₀ = 3.5 μM, [TiO₂]₀ = 875 μM (70 mg L⁻¹). *Escherichia coli* ATCC11303 was selected as the model microorganism, which was

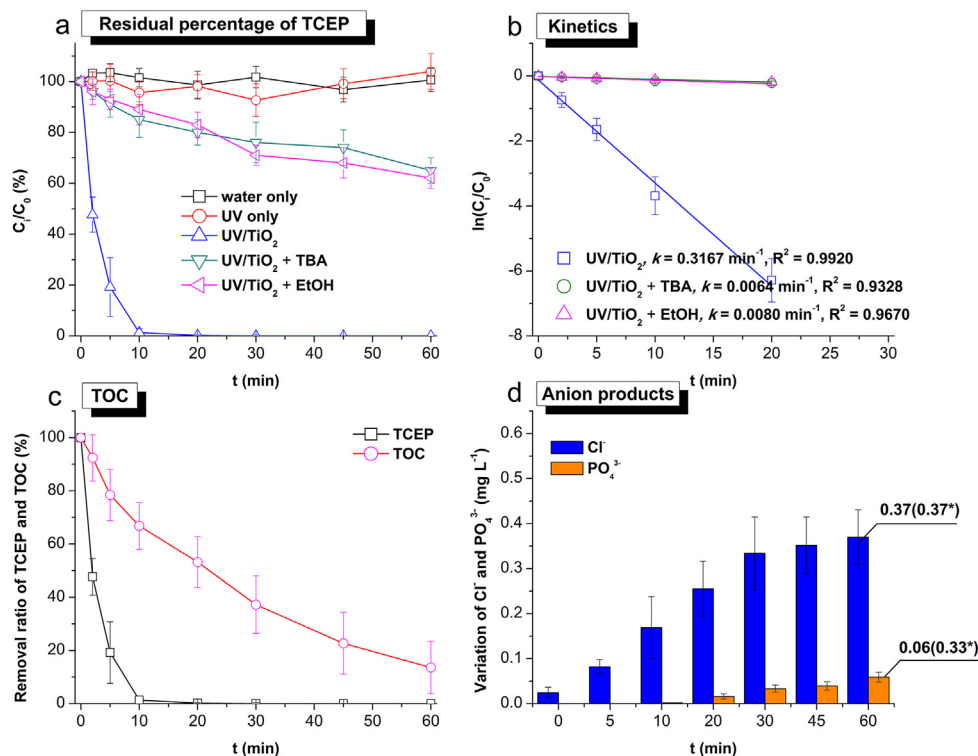


Fig. 1. Degradation efficiency of TCEP. Experimental conditions: solution temperature 25 ± 2 °C, pH 6.5–7.2, $[\text{TCEP}]_0 = 3.5$ μM , $[\text{TiO}_2]_0 = 875$ μM (70 mg L^{-1} , in UV/TiO₂ experiments). All the experiments were carried out in triplicate with error bars representing the standard error of the mean. Data with * indicate the theoretical stoichiometric amounts of PO_4^{3-} and Cl^- ions.

inoculated in LB medium at 100 r min^{-1} for 12 h. Subsequently, the cells were obtained by centrifugation at 3500g for 10 min and were washed three times. The cells (0.1 g L^{-1}) were inoculated into a 20 mL medium containing 30 mg L^{-1} KH_2PO_4 , 70 mg L^{-1} NaCl, 30 mg L^{-1} NH_4Cl , 10 mg L^{-1} MgSO_4 , 30 mg L^{-1} beef extract, 100 mg L^{-1} peptone and 1 mg L^{-1} TCEP or its intermediate mixture in dark at 25 °C on a rotary shaker at 100 r min^{-1} for 24 h. After exposure, the cells were separated and washed using phosphate buffer saline for protein extraction. The subsequent protein digestion, iTRAQ labeling and HRMS analysis followed the same procedure described in our previous research (Ou et al., 2017).

2.5. Degradation experiments in actual water matrix

The actual water matrix was collected from two different drinking water treatment plants (DWTPs) from Guangzhou City, China. The main treatment processes of these two DWTPs were: pre-chlorination (using chlorine dioxide), coagulation (using poly aluminium chloride), sedimentation, filtration and disinfection (using liquid chlorine). The source water (from Pearl River) and finished water of these two DWTPs were obtained, and the analyzed methods of water parameters are presented in Text S3. The degradation experiments using these 4 different actual water bodies as background matrixes were conducted with the initial concentration of TCEP at 3.5 μM and TiO_2 at 875 μM (70 mg L^{-1}).

3. Results and discussion

3.1. Degradation kinetics and intermediate products

The removal efficiencies of TCEP in the water-only, UV-only and UV/TiO₂ treatments are presented in Fig. 1a, while the result of TiO₂-only adsorption is showed in Fig. S2. Negligible variations of

TCEP concentration were observed both in the water-only and UV-only experiments, indicating that TCEP is stable in ultrapure water, and 254 nm irradiation cannot induce direct photolysis of TCEP. The TCEP molecule is composed of a phosphorus backbone and three chloroethane branches (Fig. S3) without any ionization. Thus, it is uncharged and maintains in a steady molecule state in water solution. Furthermore, the molar absorption coefficient of TCEP is relatively low ($\epsilon < 1000 \text{ M}^{-1} \text{ cm}^{-1}$) in the range of 240–280 nm (Fig. S3), suggesting a weak absorption of UVC irradiation. In the experiment using 254 nm UV/TiO₂, the removal effectiveness of TCEP (3.5 μM , 1 mg L^{-1}) reached ~99% after 10 min reaction ($[\text{TiO}_2]_0 = 875 \mu\text{M}$). Based on the fitting calculation, this degradation was confirmed to be a pseudo-first order reaction with an apparent rate constant (k_{obs}) at 0.3167 min^{-1} (Fig. 1b).

The fundamentals of UV/TiO₂ heterogeneous photocatalysis involve a series of chain oxidative-reductive reactions (Gaya and Abdullah, 2008):

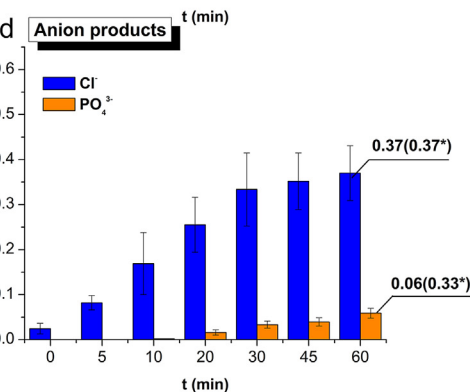
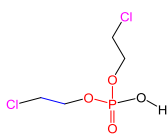
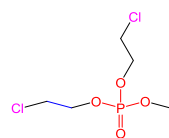
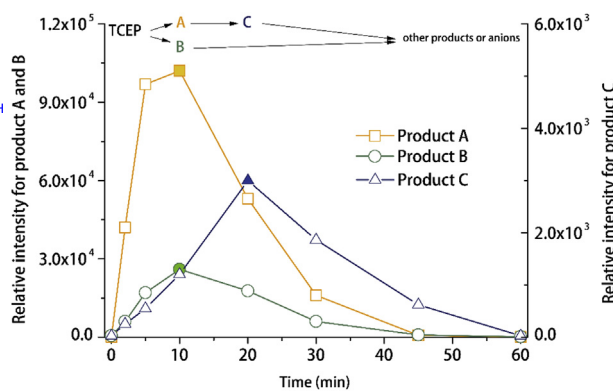
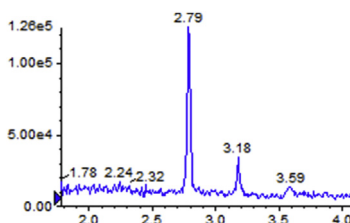
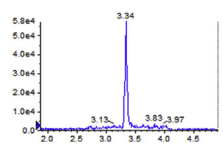
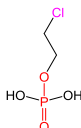
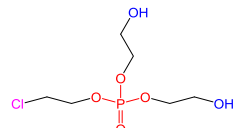
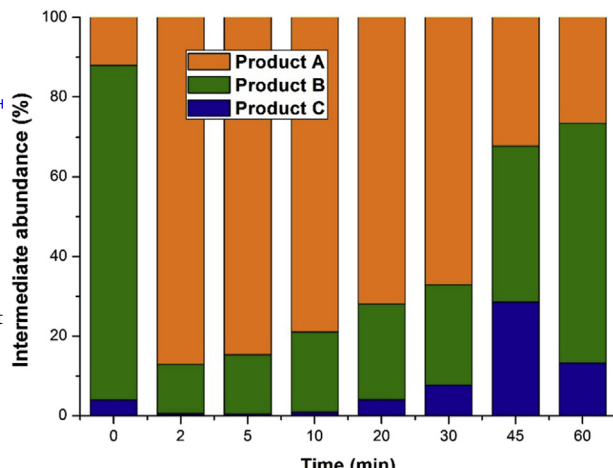
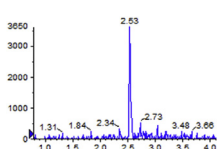


Table 1
TCEP organic intermediates in the UV/TiO₂ system.

Name	Product A	Product B	Relative intensity variations of TCEP organic intermediates
Proposed structure			
Molecular formula	C ₄ H ₉ Cl ₂ O ₄ P	C ₆ H ₁₃ Cl ₂ O ₅ P	
[M+H] ⁺ : theoretical m/z	222.9688	266.9950	
[M+H] ⁺ : observed m/z	222.9689	266.9951	
Retention time (min)	2.79	3.34	
Extracted ion chromatography			
Name	Product C	Product D	Relative abundance variations of TCEP organic intermediates
Proposed structure			
Molecular formula	C ₂ H ₆ ClO ₄ P	C ₆ H ₁₄ ClO ₆ P	
[M+H] ⁺ : theoretical m/z	160.9768	249.0289	
[M+H] ⁺ : observed m/z	160.9772	Not observed	
Retention time (min)	2.53	—	
Extracted ion chromatography		Not observed in the current experiment	

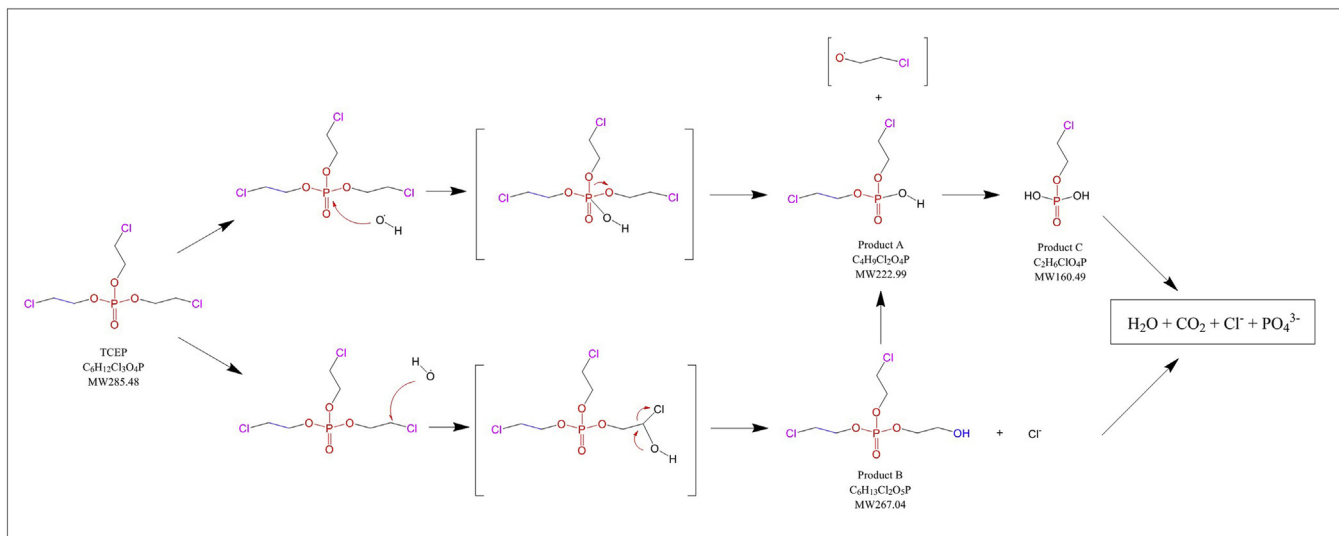
Experimental conditions: solution temperature 25 ± 2 °C, pH 6.5–7.2, [TCEP]₀ = 3.5 μM, [TiO₂]₀ = 875 μM. More detailed information of products is listed in Supplementary Materials.



To confirm the existences of active radicals (mainly $\cdot\text{OH}$), TBA and EtOH were used as scavengers. The reaction rate constants of $\cdot\text{OH}$ with TBA and EtOH were $6.0 \times 10^8 \text{ M}^{-1} \text{ s}^{-1}$ and $1.9 \times 10^9 \text{ M}^{-1} \text{ s}^{-1}$, respectively (Buxton, 1988). As showed in Fig. 1b, the k_{obs} decreased to 0.0064 min^{-1} and 0.0080 min^{-1} in the existences of TBA and EtOH, respectively, with reduction of 98% and 97% of reaction rate. This result indicated that the degradation was severely inhibited, and $\cdot\text{OH}$ oxidation might be the dominating reaction mechanism. Furthermore, the result of adsorption experiment suggested that TiO₂ had a negligible adsorption of TCEP under different pH values (Fig. S2). Therefore, all these results evidenced that active radicals contributed to the degradation of TCEP in UV/TiO₂ system.

The variation of TOC is showed in Fig. 1c. The theoretical TOC value is $0.25 \pm 0.03 \text{ mg L}^{-1}$ for the 3.5 μM TCEP solution. Only 45% TOC was removed when the removal efficiency of TCEP reached nearly 100% after 20-min reaction, suggesting an incomplete degradation. On the other hand, the evolution tendency of PO₄³⁻ also supported this conclusion. Theoretically, 3.5 μM TCEP contains approximate $0.37 \text{ mg L}^{-1} \text{ Cl}^-$ and $0.33 \text{ mg L}^{-1} \text{ PO}_4^{3-}$. After 60-min reaction, the observed Cl⁻ was equal to the stoichiometric amount, indicating a complete dechlorination (Fig. 1d). But the observed PO₄³⁻ dosage at 0.06 mg L^{-1} was lower than the stoichiometric amount, suggesting an incomplete transformation of TCEP backbone, which would generate various intermediates. These results were consistent with the research focused on the degradation of TCPP, which reported a similar rapid release of Cl⁻ and a slow release of PO₄³⁻ (Antonopoulou et al., 2016).

The screening of potential intermediates from the HRMS data was performed based on the possible transformations of TCEP. Two sites in TCEP, including the C–Cl bond and the central phosphate (Fig. S3), may be attacked by the active radical species. After



Scheme 1. Proposed generative pathways of degrading products from TCEP in 254 nm UV/TiO₂ system. Brackets indicate the structures expected, but not detected during experiment.

screening, three steady intermediates were confirmed, including C₄H₉Cl₂O₄P (product A, *m/z* 222.9689), C₆H₁₃Cl₂O₅P (product B, *m/z* 266.9951) and C₂H₆ClO₄P (product C, *m/z* 160.9772). The MS² spectra of these products are presented in Figs. S4–S6. The detailed information and relative intensity variations of these intermediates are presented in Table 1. As •OH was confirmed to be the dominating attacking radical in the UV/TiO₂ system, generating pathways of intermediates were proposed based on •OH oxidation (Scheme 1). Generally, •OH can abstract H from C–H bonds, and this can result in the formation of different products.

Product A (Fig. S4) has a MW of 222.99 Da, which is formed through the cleavage of an ethyl-chlorine arm from the phosphoric center. The generating pathway of product A may involve a two-step reaction (Scheme 1). First, a •OH attacked the phosphoric center, resulting in an addition. Second, a cleavage of one oxygen-ethyl-chlorine arm occurred and left behind product A. The further reaction of product A following the same pattern will form product C (Fig. S5), which has a MW of 160.49. After three cycles of this reaction, a TCEP molecule can be degraded to one phosphate radical and other further products.

Product B (Fig. S6) has a MW of 267.04 Da, and it has a substitution of one chlorine terminal by a hydroxyl. The generating pathway of product B, which may also involve an addition, substitution and rupture process induced by •OH (Scheme 1). Of note, product D, which was expected to be the further oxidized intermediate of product B, was not observed in the current reaction. Similar alterations of TCPP were reported, and the principal photocatalytic transformation routes were also confirmed to be hydroxylation, oxidation, dechlorination and dealkylation (Antonopoulou et al., 2016).

The relative intensity and abundance variations are presented in Table 1. The intensity of product A increased to approximate 1.0×10^5 at 10 min and then showed a decreasing tendency. The intensity of product B showed a similar pattern with a maximum intensity of 2.6×10^4 at 10 min. Furthermore, the variation of product C was relative moderate, which increased to 3.0×10^3 at 20 min, and then decreased slowly within 60 min. These results confirmed the proposed generative pathway from product A to product C. Of note, product A was dominating in terms of the relative intensity during the early stage of reaction (0–30 min), and the abundances of products B and C continued to increase when

degradation proceeded (30–60 min), with the synchronous generations of other further degrading products.

3.2. Differential protein expression and safety evaluation

To date, some approaches used to evaluate the toxicology of OPEs and their degradation products were primarily based on the phenotype change. For example, the products of TCPP during UV/TiO₂ treatment were found to exhibit decreasing inhibition on the *Vibrio Fischeri* luminescence (Antonopoulou et al., 2016). A phenotype result from the expression of a genetic code via a multi-step process can determine whether the general toxicity of the degrading products on a specific organism decreased or not, but they could not reflect the intrinsic interaction between degrading products and cellular proteome. To this end, a proteome analysis was required.

The degrading intermediate mixtures at 10 min and 45 min were obtained in the current study for the exposed experiments of *E. coli* ATCC11303. In the early stage of TCEP degradation (~10 min), nearly 99% TCEP was transformed to preliminary degrading products, such as product A, whereas, other further degrading products were dominating in the later stage of reaction (45 min). Therefore, the general toxicities and biomolecular interaction of products in different degrading stages can be compared. The intermediate mixture generated in the early stage caused 360 proteins significantly differential expressed, whereas, those intermediates produced in the later stage triggered 319 proteins up- and down-regulated synthesis (Table S3).

To clarify the impact of intermediate mixture on cellular metabolic network, the metabolic reactions catalyzed by the differentially synthesized proteins were mapped in the Kyoto Encyclopedia of Genes and Genomes network database (Fig. 2). The red lines those connected different cellular metabolic products stand for the reactions catalyzed by the up-regulated proteins, whereas, the black lines represent the reactions catalyzed by the down-regulated enzymes. According to the mapped results (the red network shown in Fig. 2), 194 up-regulated expression proteins, which extracted from the cells under the exposure to 10-min TCEP intermediates compared to TCEP, primarily participated in TCA cycle, oxidative phosphorylation, biotin metabolism, carbohydrate (fructose and mannose) metabolism, fatty acid biosynthesis, amino

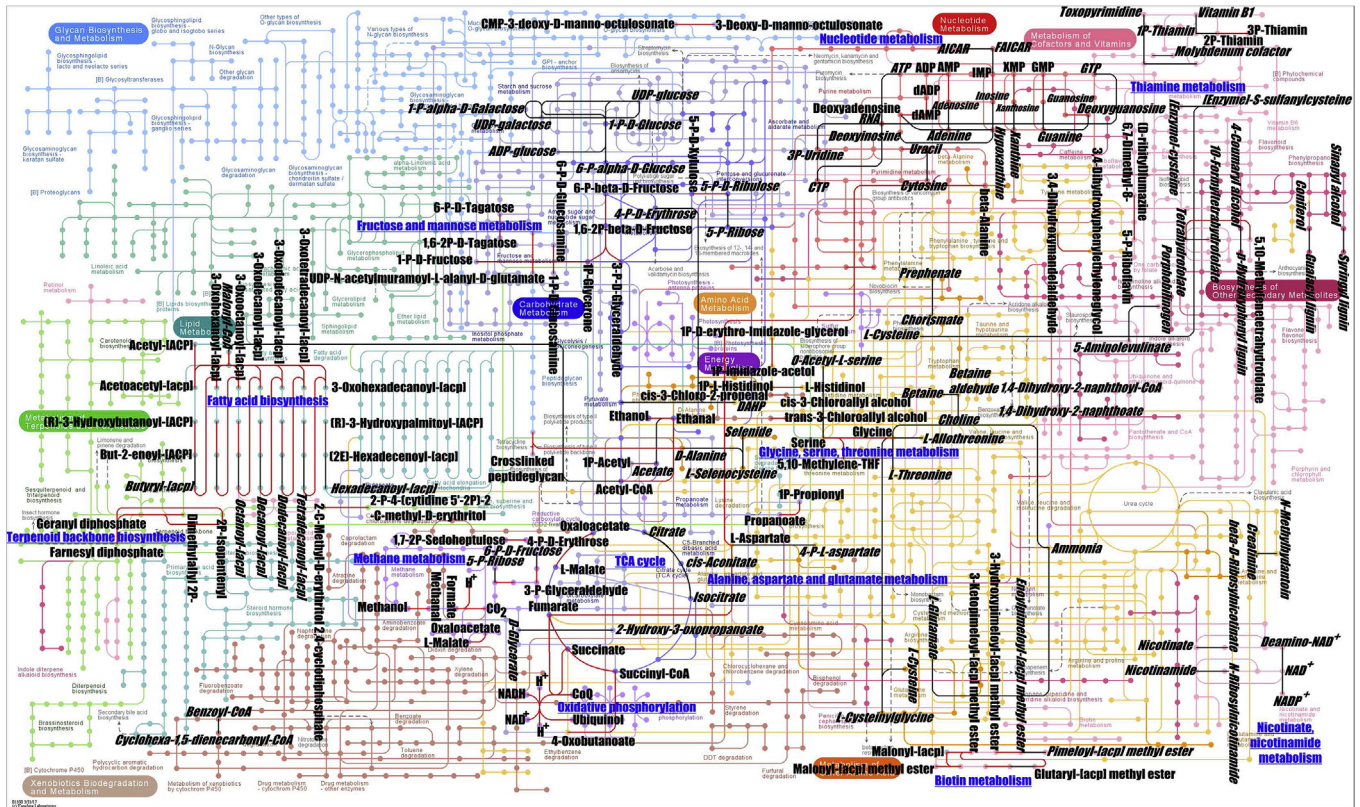


Fig. 2. The KEGG metabolism network related to the different regulated expression proteins in cells under the exposure to 10-min TCEP intermediate mixture compared to TCEP. Red line indicates the up-regulated metabolism pathway, while the black line indicates the down-regulated metabolism pathway. (For interpretation of the references to colour in this figure legend, the reader is referred to the web version of this article.)

acid (glycine, serine, alanine and aspartate) metabolism, ATP and nucleotide metabolism, and terpenoid backbone biosynthesis. Although the down-regulated expression proteins were also participated in the similar pathways, they were associated with different reactions in the same network (the black network shown in Fig. 2).

Fumarate, succinate, malate and oxaloacetate were accumulated in the TCA cycle, whereas, citrate and isocitrate were consumed; unsaturated fatty acids in fatty acid biosynthesis pathway were up-generated by using the saturated ones. The down-expression of superoxide dismutases SodB and SodC, universal stress protein UspD, stringent starvation protein sspA, and acid stress chaperones HdeA and HdeB inferred that the toxicity of intermediates is significant lower than TCEP (Fig. S7) (Roh et al., 2009; Zhang et al., 2011).

Proteins rarely act alone as their functions tend to be regulated by protein–protein interactions, which are the physical contacts with high specificity established between proteins. Therefore, protein–protein interaction is an important perspective to reveal the biomolecule impact of TCEP and its intermediates at proteomic level. The consistency between protein interaction network (Fig. 3) and metabolic network (Fig. 2) confirmed that proteomic technology is an insightful and useful approach to investigate impacts of target compounds on biomolecule network. Several key node proteins, including Adk, AtpA, AtpD, AtpF, DnaK, GroS and GapA, connected the ribosome pathway, carbon metabolism, glycolysis/gluconeogenesis pathway, TCA cycle and amino acid biosynthesis. Among these proteins, AtpA, AtpD and AtpF are the regulatory subunit, catalytic site subunit and synthase subunit of the ATP synthase responsible for ATP production (Lopez-Gallardo et al.,

2016). AtpF contains an extramembranous catalytic core and a membrane proton channel, which linked together by a central stalk and a peripheral stalk. Its up-synthesis is consistent with the enhanced expression of DnaK, GroS and Adk, which acted as a chaperone, co-chaperonin and adenylate kinase (Cao et al., 2017; Kaur et al., 2016), respectively, associating with the transport of materials, and the reversible transfer of the terminal phosphate group between ATP and AMP. The current significant activation of transmembrane transport and energy generation meant that TCEP intermediate mixture could be transported and utilized through cellular metabolism, and its toxicity was obviously lower than TCEP. The above findings confirmed that complete mineralization of TCEP is unnecessary using UV/TiO₂ treatment since its intermediates produced in the early stage can be further degraded safely by bacteria who are the major group of organisms in the natural ecosystems; proteomic approach can be an insightful and novel tool for evaluating the phylogenetic risk of various compounds and water treatment technologies at system level of cellular metabolism networks and functional protein association networks.

The molecular function of ribosome, linking amino acids together in the order specified by mRNA molecules to form proteins, explained why glycine, serine, alanine, aspartate, ATP and nucleotide metabolism was up-regulated. Cells under the exposure to 45-min TCEP intermediate mixture exhibited the similar metabolism networks, whereas, oxidative phosphorylation was down expressed (Fig. 2). In comparison to the stress of 10-min TCEP intermediates, this finding confirmed that less energy was generated to utilize further degrading products of TCEP in the later stage.

The terpenoid backbone biosynthesis and the reversible transformation of D-ribose 5 phosphate to D-ribulose 5 phosphate,

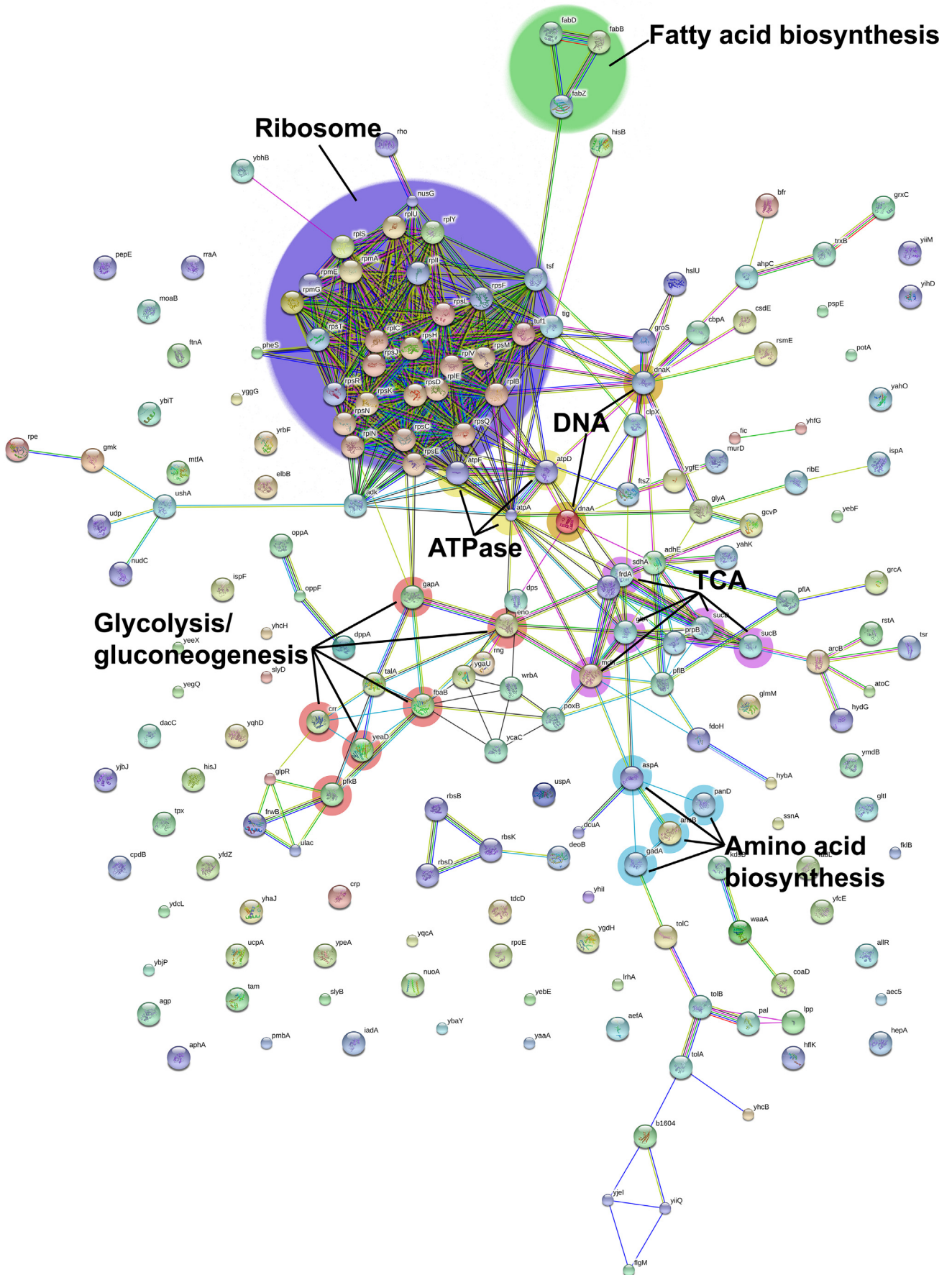
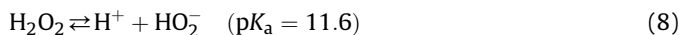


Fig. 3. The interaction among the up-regulated expression proteins in cells under the exposure to 10-min TCEP intermediate mixture compared to TCEP.

aldehyde to acetate, prephenate to chorismate, D-glutamate to D-glutamine, tetrahydrofolate to 10-formyltetrahydrofolate, and inosinic acid to 5-aminoimidazole-4-carboxamide ribotide did not exhibit significant alteration in cells under the stress of 45-min TCEP intermediates (Fig. S8). The reduction of metabolism reactions, pathways and network related to resist, transport and utilize the intermediate products generated in this stage exhibited the decreasing risk of them.

3.3. Influence factors

Quantification of the influence of quality feature and coexisting contaminants in background water is essential to determine the level of their interference, further to assess the feasibility of UV/TiO₂. In heterogeneous photocatalytic systems, pH is one of the most important operating parameters that affects the charge on the catalyst particles, size of catalyst aggregates and the entire oxidative-reductive reaction chain (Meng et al., 2010). Normally, the effect of pH on photocatalysis degradation can be explained by taking into consideration the properties of both catalyst and contaminant at different pH values. The surface charge of TiO₂ changes from positive ($pK_{a1} = 2.6$) to negative ($pK_{a2} = 9.0$) with point of zero at pH 6.4, but TCEP maintains in molecule state without ionization under different pH condition. In addition, no adsorption of TCEP onto TiO₂ was observed under pH values in the range of 3.0–11.0 (Fig. S2). Therefore, pH variation may mainly affect the characteristic of TiO₂ and its derived chain oxidative-reductive reactions (Eqs. (1)–(7)). The highest k_{obs} was observed under neutral condition (pH = 7.0), and it decreased when pH increased or decreased (Fig. 4). In the acidic condition, the excess H⁺ and insufficient OH⁻ impeded the direct generation of •OH from h⁺ (Eq. (3)). The accumulation of h⁺ on the surface of TiO₂ inhibited the further photo activation of TiO₂ (Eq. (1)), and the entire degradation rate of TCEP decreased. This inhibition was intensified when pH further decreased. In the alkaline condition, the insufficient H⁺ also impeded the generation of H₂O₂ (Eqs. (4) and (6)), resulting in a similar chain inhibition on reaction. Furthermore, since pH 11 was close to the pK_a of H₂O₂ (Eq. (8)) (Crittenden et al., 1999), the deprotonation of H₂O₂ induced the formation of HO₂⁻, which became another competitive target for •OH (Eq. (9)). Therefore, the neutral condition (pH = ~7.0) was conducive to the TCEP degradation using UV/TiO₂, while acidic and alkaline conditions should be avoided.



The presences of anions and NOM in natural water for TiO₂ photocatalytic treatment were expected, and related photocatalyst fouling and deactivation were usually observed. Therefore, typical photocatalysis inhibitors, including Cl⁻, NO₃⁻ and humic acid, were selected to test their influences. As shown in Fig. S9, the k_{obs} decreased from 0.3232 min⁻¹ (control) to 0.0120 min⁻¹ (100 mg L⁻¹ Cl⁻), 0.0695 min⁻¹ (100 mg L⁻¹ NO₃⁻) and 0.0045 min⁻¹ (100 mg L⁻¹ humic acid), respectively. The inhibition mechanism of Cl⁻ on UV/TiO₂ via radicals and holes scavenging may involve the following reactions (Meng et al., 2010):



The adsorption of Cl⁻ onto the TiO₂ surface was preferential, and it would reduce the generating amount of •OH, resulting in inhibition of photocatalysis. The effects of NO₃⁻ on the reaction rate depended on NO₃⁻ concentration. Low concentration NO₃⁻ (1 mg L⁻¹) enhanced the reaction rate of TCEP as a result of NO₃⁻ photolysis to produce •OH (Wang et al., 2012). But for high concentration NO₃⁻ (>10 mg L⁻¹), UV screening may be the primary mechanism, which reduced the photo-quantum yield in the UV/TiO₂ system (Wang et al., 2012). Quantum yield decreased as a result of the direct competition of inorganic ions for light photons, which reduced the whole reaction rate. Humic acid also had a UV screening effect, and it had a competitive reaction with •OH, resulting in a decrease of the reaction rate. Similar inhibition phenomena were observed in the studies conducted by Xiao et al., (2016), Liao et al., (2016), and Sharma et al., (2015), which also investigated the removal of targeted contaminants by •OH method with humic acid. Thus, the determination of the amounts of inorganic ions and humic acid in targeted water body is an important issue for the successful implementation of TiO₂ photocatalytic treatment.

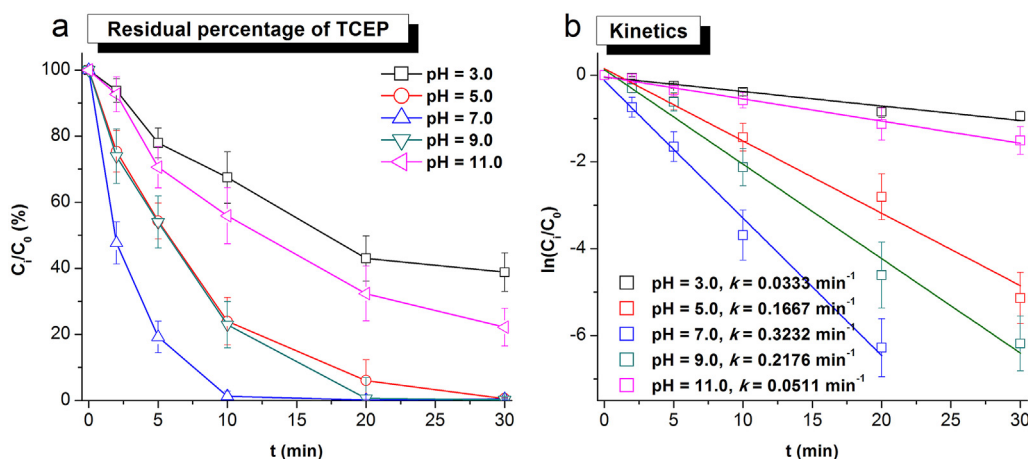


Fig. 4. Influence of different pH in UV/TiO₂ experiments. Experimental conditions: solution temperature 25 ± 2 °C, [TCEP]₀ = 3.5 μM, [TiO₂]₀ = 875 μM (70 mg L⁻¹). All the experiments were carried out in triplicate with error bars representing the standard error of the mean.

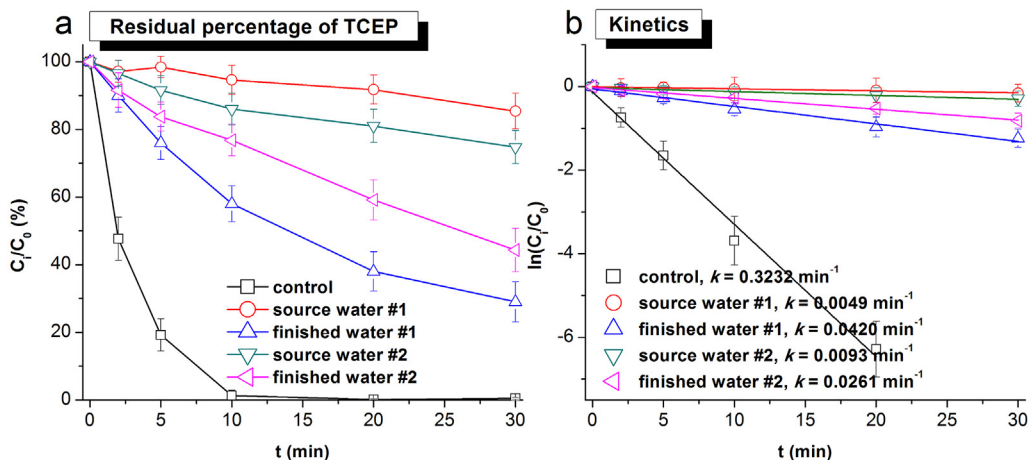


Fig. 5. Degradation of TCEP in natural source water and finished water. Experimental conditions: solution temperature $25 \pm 2 \text{ }^\circ\text{C}$, $[\text{TCEP}]_0 = 3.5 \text{ }\mu\text{M}$, $[\text{TiO}_2]_0 = 875 \text{ }\mu\text{M}$ (70 mg L^{-1}). All the experiments were carried out in triplicate with error bars representing the standard error of the mean.

3.4. Degradation of TCEP in actual water matrix

The water quality parameters of actual water matrix are listed in Table S4 and S5, and the degradation efficiencies of TCEP in these matrixes are presented in Fig. 5. The k_{obs} significantly decreased from 0.3232 min^{-1} to 0.0420 min^{-1} (finished water #1) and 0.0261 min^{-1} (finished water #2) using two finished water matrixes, but for the systems using source waters, the inhibition was severer, with the k_{obs} at 0.0049 min^{-1} (source water #1) and 0.0093 min^{-1} (source water #2). Based on the results of “Influence factors” (Section 3.3), the degradation can be affected by NOM and anions. As showed in Tables S4 and S5, two source water matrixes contained more NOM (TOC), especially aromatic organic matters (UV_{254}), than corresponding finished waters. And the concentrations of most anions (Cl^- , SO_4^{2-} and NO_3^-) in the source waters were higher than those in the finished waters (Table S5). Thus, the source waters had more negative impacts on TCEP degradation than the finished waters.

3.5. Cost evaluation

The electrical energy per order (EE/O) value was used to evaluate the electrical cost of reactions. The EE/O is defined as the electrical energy in kilowatt per hours (kWh) required to degrade a specific contaminant by one order of magnitude in 1 m^3

contaminated water or air. The detailed calculation procedure was reported in Ref. (He et al., 2013). Generally, EE/O can be calculated using Eq. (12):

$$\text{EE/O}_{\text{-uv}} = \frac{P \times t}{V \times \lg\left(\frac{C_i}{C_f}\right)} \quad (12)$$

where, $\text{EE/O}_{\text{-uv}}$ has the unit of $\text{kWh m}^{-3} \text{ order}^{-1}$; P is the total electrical power or flux to drive UV irradiation entering the reactor, kW; t is the time which 90% of TCEP is removed, h; V indicates the volume of the given reaction system, m^3 ; C_i is the initial concentration of the targeted contaminant, mg L^{-1} ; C_f is the final concentration of the targeted contaminant, mg L^{-1} . The results are presented in Table 2. The $\text{EE/O}_{\text{-uv}}$ values in the $254 \text{ nm UV} + 875 \text{ }\mu\text{M TiO}_2$ system were $0.0113 \text{ kWh m}^{-3} \text{ order}^{-1}$. For the influence factor experiments, EE/O values increased when k_{obs} decreased. The EE/O values significantly increased under $\text{pH} = 3.0$, $\text{pH} = 11.0$, additions of anions and humic acid. Of note, the EE/O values increased to $0.7310 \text{ kWh m}^{-3} \text{ order}^{-1}$ and $0.3851 \text{ kWh m}^{-3} \text{ order}^{-1}$, respectively, when using source water matrixes #1 and #2. For finished waters, the EE/O values dramatically decreased to $0.0853 \text{ kWh m}^{-3} \text{ order}^{-1}$ (#1) and $0.1372 \text{ kWh m}^{-3} \text{ order}^{-1}$ (#2), suggesting that the removal of coexisting NOM and anions was conducive to the TCEP degradation, and the conventional drinking water treatment

Table 2
EE/O values for TCEP degradation in UV/TiO₂ system.

System	P (kW)	k_{obs} (h^{-1})	t_1 (h)	Pt (kWh)	V (m^3)	EE/O _{-uv}
pH = 3.0	5.6×10^{-4}	0.0333	1.15	0.000645	1.0×10^{-4}	0.1076
pH = 5.0	5.6×10^{-4}	0.1667	0.23	0.000129	1.0×10^{-4}	0.0215
pH = 7.0 (control)	5.6×10^{-4}	0.3232	0.12	0.000068	1.0×10^{-4}	0.0113
pH = 9.0	5.6×10^{-4}	0.2176	0.18	0.000099	1.0×10^{-4}	0.0165
pH = 11.0	5.6×10^{-4}	0.0511	0.75	0.000421	1.0×10^{-4}	0.0701
Cl^- (100 mg L^{-1})	5.6×10^{-4}	0.012	3.20	0.001791	1.0×10^{-4}	0.2985
Humic acid (100 mg L^{-1})	5.6×10^{-4}	0.0045	8.53	0.004776	1.0×10^{-4}	0.7960
NO_3^- (100 mg L^{-1})	5.6×10^{-4}	0.0695	0.55	0.000309	1.0×10^{-4}	0.0515
Source water #1	5.6×10^{-4}	0.0049	7.83	0.004386	1.0×10^{-4}	0.7310
Finished water #1	5.6×10^{-4}	0.042	0.91	0.000512	1.0×10^{-4}	0.0853
Source water #2	5.6×10^{-4}	0.0093	4.13	0.002311	1.0×10^{-4}	0.3851
Finished water #2	5.6×10^{-4}	0.0261	1.47	0.000823	1.0×10^{-4}	0.1372

Experimental conditions: solution temperature $25 \pm 2 \text{ }^\circ\text{C}$, $\text{pH} 6.5\text{--}7.2$, $[\text{TCEP}]_0 = 3.5 \text{ }\mu\text{M}$, $[\text{TiO}_2]_0 = 875 \text{ }\mu\text{M}$ (if not be specified).

P is the total electrical power or flux to drive UV irradiation entering the reactor (kW), V is the volume (m^3) of the given reaction system, t_1 is the time (h) which 90% of TCEP is removed.

The unit of EE/O is $\text{kWh m}^{-3} \text{ order}^{-1}$.

processes followed by a UV/TiO₂ treatment would be feasible.

4. Conclusion

The degradation of TCEP using UV/TiO₂ heterogeneous photocatalysis followed a pseudo-first order reaction with a k_{obs} of 0.3167 min⁻¹, and •OH oxidation was confirmed to be the dominating degrading mechanism. The neutral condition was conducive to the TCEP degradation using UV/TiO₂, while the existences of Cl⁻, NO₃⁻ and humic acid had negative effects on the reaction. The natural source water which was rich in NOM and anions also affected the degradation efficiency significantly, while the finished water after conventional drinking water treatment processes had less impact on TCEP degradation.

As the reaction proceeded, TCEP was transformed to several preliminary hydroxylated and dechlorinated products in the early stage, followed by the generation of distinct further degrading products in the later stage. Based on the proteomics analysis, the significant activation of transmembrane transport and energy generation suggested that these degrading products can be transported and utilized through cellular metabolism, and their toxicity was obviously weakened and decreased. In conclusion, incomplete hydroxylation and dechlorination of TCEP was normal during UV/TiO₂ treatment, and it was effective for its detoxification.

Acknowledgments

This project was supported by the National Natural Science Foundation of China (Grant Nos. 51308224, 21577049), the Science and Technology Planning Project of Guangdong Province, China (Grant No. 2014A020216014).

Appendix A. Supplementary data

Supplementary data related to this article can be found at <http://dx.doi.org/10.1016/j.watres.2017.07.034>.

References

- Alvarez-Corena, J.R., Bergendahl, J.A., Hart, F.L., 2016. Photocatalytic oxidation of five contaminants of emerging concern by UV/TiO₂: identification of intermediates and degradation pathways. *Environ. Eng. Sci.* 33 (2), 140–147.
- Antonopoulou, M., Giannakas, A., Bairamis, F., Papadaki, M., Konstantinou, I., 2017. Degradation of organophosphorus flame retardant tris (1-chloro-2-propyl) phosphate (TCPP) by visible light N,S-codoped TiO₂ photocatalysts. *Chem. Eng. J.* 318, 231–239.
- Antonopoulou, M., Karagianni, P., Konstantinou, I.K., 2016. Kinetic and mechanistic study of photocatalytic degradation of flame retardant Tris (1-chloro-2-propyl) phosphate (TCPP). *Appl. Catal. B Environ.* 192, 152–160.
- Bergman, A., Rydén, A., Law, R.J., Boer, J.D., Covaci, A., Alaee, M., Birnbaum, L., Petreas, M., Rose, M., Sakai, S., 2012. A novel abbreviation standard for organobromine, organochlorine and organophosphorus flame retardants and some characteristics of the chemicals. *Environ. Int.* 49C, 57–82.
- Buxton, G.V., 1988. Critical Review of rate constants for reactions of hydrated electrons, hydrogen atoms and hydroxyl radicals (•OH/•O) in aqueous solution. *J. Phys. Chem. Refer. Data* 17 (2), 513–886.
- Cao, H., Wei, D., Yang, Y., Shang, Y., Li, G., Zhou, Y., Ma, Q., Xu, Y., 2017. Systems-level understanding of ethanol-induced stresses and adaptation in *E. coli*. *Sci. Rep.* 7, 44150.
- Crittenden, J.C., Hu, S., Hand, D.W., Green, S.A., 1999. A kinetic model for H₂O₂/UV process in a completely mixed batch reactor. *Water Res.* 33 (10), 2315–2328.
- Dodd, M.C., Kohler, H.-P.E., Von Gunten, U., 2009. Oxidation of antibacterial compounds by ozone and hydroxyl radical: elimination of biological activity during aqueous ozonation processes. *Environ. Sci. Technol.* 43 (7), 2498–2504.
- Gaya, U.I., Abdullah, A.H., 2008. Heterogeneous photocatalytic degradation of organic contaminants over titanium dioxide: a review of fundamentals, progress and problems. *J. Photochem. Photobiol. C Photochem. Rev.* 9 (1), 1–12.
- He, X., Cruz, A.A.D.L., Dionysiou, D.D., 2013. Destruction of cyanobacterial toxin cylindrospermopsin by hydroxyl radicals and sulfate radicals using UV-254 nm activation of hydrogen peroxide, persulfate and peroxymonosulfate. *J. Photochem. Photobiol. A Chem.* 251 (48), 160–166.
- Kasprzyk-Hordern, B., Ziolek, M., Nawrocki, J., 2003. Catalytic ozonation and methods of enhancing molecular ozone reactions in water treatment. *Appl. Catal. B-Environ.* 46 (4), 639–669.
- Kaur, H., Lakatos-Karoly, A., Vogel, R., Noll, A., Tampe, R., Glaubitz, C., 2016. Coupled ATPase-adenylate kinase activity in ABC transporters. *Nat. Commun.* 7, 13864.
- Kim, S., Jung, J., Lee, I., Jung, D., Youn, H., Choi, K., 2015. Thyroid disruption by triphenyl phosphate, an organophosphate flame retardant, in zebrafish (*Danio rerio*) embryos/larvae, and in GH3 and FRTL-5 cell lines. *Aquat. Toxicol.* 160, 188–196.
- Liao, Q.N., Ji, F., Li, J.C., Zhan, X.M., Hu, Z.H., 2016. Decomposition and mineralization of sulfaquinoxaline sodium during UV/H₂O₂ oxidation processes. *Chem. Eng. J.* 284, 494–502.
- Lopez-Gallardo, E., Llobet, L., Emperador, S., Montoya, J., Ruiz-Pesini, E., 2016. Effects of tributyltin chloride on cybrids with or without an ATP synthase pathologic mutation. *Environ. Health Perspect.* 124 (9), 1399–1405.
- Meng, N.C., Bo, J., Chow, C.W.K., Saint, C., 2010. Recent developments in photocatalytic water treatment technology: a review. *Water Res.* 44 (10), 2997–3027.
- Ou, H.S., Liu, J., Ye, J.S., Wang, L.L., Gao, N.Y., Ke, J., 2017. Degradation of tris(2-chloroethyl) phosphate by ultraviolet-persulfate: kinetics, pathway and intermediate impact on proteome of *Escherichia coli*. *Chem. Eng. J.* 308, 386–395.
- Pillai, S.C., Stangar, U.L., Byrne, J.A., Perez-Larios, A., Dionysiou, D.D., 2015. Photocatalysis for disinfection and removal of contaminants of emerging concern. *Chem. Eng. J.* 261, 1–2.
- Reemtsma, T., Quintana, J.B., Rodil, R., Garcá, M., Rodri, I., 2008. Organophosphorus flame retardants and plasticizers in water and air I. Occurrence and fate. *Trends Anal. Chem.* 27 (9), 727–737.
- Roh, J.Y., Sim, S.J., Yi, J., Park, K., Chung, K.H., Ryu, D.Y., Choi, J., 2009. Ecotoxicity of silver nanoparticles on the soil nematode *caenorhabditis elegans* using functional ecotoxicogenomics. *Environ. Sci. Technol.* 43 (10), 3933–3940.
- Ruan, X.C., Ai, R., Jin, X., Zeng, Q.F., Yang, Z.Y., 2013. Photodegradation of tri(2-chloroethyl) phosphate in aqueous solution by UV/H₂O₂. *Water, Air, & Soil Pollut.* 224 (1), 1–10.
- Santoro, D., Raisee, M., Moghaddami, M., Ducoste, J., Sasges, M., Liberti, L., Notarnicola, M., 2010. Modeling hydroxyl radical distribution and trialkyl phosphates oxidation in UV-H₂O₂ photoreactors using computational fluid dynamics. *Environ. Sci. Technol.* 44 (16), 6233–6241.
- Sharma, J., Mishra, I.M., Kumar, V., 2015. Degradation and mineralization of Bisphenol A (BPA) in aqueous solution using advanced oxidation processes: UV/H₂O₂ and UV/S₂O₈²⁻ oxidation systems. *J. Environ. Manag.* 156, 266–275.
- Stackelberg, P.E., Furlong, E.T., Meyer, M.T., Zaugg, S.D., Henderson, A.K., Reissman, D.B., 2004. Persistence of pharmaceutical compounds and other organic wastewater contaminants in a conventional drinking-water-treatment plant. *Sci. Total Environ.* 329 (1–3), 99–113.
- Ta, N., Li, C., Fang, Y., Liu, H., Lin, B., Jin, H., Tian, L., Zhang, H., Zhang, W., Xi, Z., 2014. Toxicity of TDCPP and TCEP on PC12 cell: changes in CAMKII, GAP43, tubulin and NF-H gene and protein levels. *Toxicol. Lett.* 227 (3), 164–171.
- van der Veen, I., de Boer, J., 2012. Phosphorus flame retardants: properties, production, environmental occurrence, toxicity and analysis. *Chemosphere* 88 (10), 1119–1153.
- Waaijers, S.L., Hartmann, J., Soeter, A.M., Helmus, R., Kools, S.A., de Voegt, P., Admiraal, W., Parsons, J.R., Kraak, M.H., 2013. Toxicity of new generation flame retardants to *Daphnia magna*. *Sci. Total Environ.* 463, 1042–1048.
- Wang, C.Y., Zhu, L.Y., Wei, M.C., Chen, P., Shan, G.Q., 2012. Photolytic reaction mechanism and impacts of coexisting substances on photodegradation of bisphenol A by Bi₂WO₆ in water. *Water Res.* 46 (3), 845–853.
- Watts, M.J., Linden, K.G., 2008. Photooxidation and subsequent biodegradability of recalcitrant tri-alkyl phosphates TCEP and TBP in water. *Water Res.* 42 (20), 4949–4954.
- Wei, G.L., Li, D.Q., Zhuo, M.N., Liao, Y.S., Xie, Z.Y., Guo, T.L., Li, J.J., Zhang, S.Y., Liang, Z.Q., 2015. Organophosphorus flame retardants and plasticizers: sources, occurrence, toxicity and human exposure. *Environ. Pollut.* 196, 29–46.
- Wolschke, H., Suhring, R., Xie, Z.Y., Ebinghaus, R., 2015. Organophosphorus flame retardants and plasticizers in the aquatic environment: a case study of the Elbe River, Germany. *Environ. Pollut.* 206, 488–493.
- Xiao, Y.J., Zhang, L.F., Zhang, W., Lim, K.Y., Webster, R.D., Lim, T.T., 2016. Comparative evaluation of iodoacids removal by UV/persulfate and UV/H₂O₂ processes. *Water Res.* 102, 629–639.
- Ye, J.S., Liu, J., Ou, H.S., Wang, L.L., 2016. Degradation of ciprofloxacin by 280nm ultraviolet-activated persulfate: degradation pathway and intermediate impact on proteome of *Escherichia coli*. *Chemosphere* 165, 311–319.
- Yuan, X., Lacorte, S., Cristale, J., Dantas, R.F., Sans, C., Espugas, S., Qiang, Z., 2015. Removal of organophosphate esters from municipal secondary effluent by ozone and UV/H₂O₂ treatments. *Sep. Purif. Technol.* 156, 1028–1034.
- Zhang, M., Lin, S.X., Song, X.W., Liu, J., Fu, Y., Ge, X., Fu, X.M., Chang, Z.Y., Chen, P.R., 2011. A genetically incorporated crosslinker reveals chaperone cooperation in acid resistance. *Nat. Chem. Biol.* 7 (10), 671–677.